

Shaping mmWave Wireless Channel via Multi-Beam Design using Reconfigurable Intelligent Surfaces

Nariman Torkzaban
University of Maryland, College Park
College Park, MD
narimant@umd.edu

Mohammad A. (Amir) Khojastepour
NEC Laboratories, America
Princeton, NJ
amir@nec-labs.com

Abstract—Millimeter-wave (mmWave) communications is considered as a key enabler towards the realization of next-generation wireless networks, due to the abundance of available spectrum at mmWave frequencies. However, mmWave suffers from high free-space path-loss and poor scattering resulting in mostly line-of-sight (LoS) channels which result in a lack of coverage. Reconfigurable intelligent surfaces (RIS), as a new paradigm, have the potential to fill the coverage holes by shaping the wireless channel. In this paper, we propose a novel approach for designing RIS with elements arranged in a uniform planar array (UPA) structure. In what we refer to as multi-beamforming, We propose and design RIS such that the reflected beam comprises multiple disjoint lobes. Moreover, the beams have optimized gain within the desired angular coverage with fairly sharp edges avoiding power leakage to other regions. We provide a closed-form low-complexity solution for the multi-beamforming design. We confirm our theoretical results by numerical analysis.

Index Terms—Beamforming, Reconfigurable Intelligent Surface (RIS), Uniform Planar Array (UPA), Blind-spot, MIMO

I. INTRODUCTION

Next generation of wireless communication systems aims to address the ever-increasing demand for high throughput, low latency, better quality of service and ubiquitous coverage. The abundance of bandwidth available at the mmWave frequency range, i.e., [20, 100] Ghz, is considered as a key enabler towards the realization of the promises of next generation wireless communication systems. However, communication in mmWave suffers from high path-loss, and poor scattering. Since the channel in mmWave is mostly LoS, i.e., a strong LoS path and very few and much weaker secondary components, the mmWave coverage map includes *blind spots* as a result of shadowing and blockage. Beamforming is primarily used to address the high attenuation in the channel. In addition to beamforming, relaying can potentially be designed to generate constructive superposition and enhance the received signals at the receiving nodes. Reconfigurable intelligent surface (RIS)[1][2][3] is a new paradigm with a great potential for stretching the coverage and enhancing the capacity of next-generation communication systems. Indeed, it is possible to shape the wireless channel by using RIS, e.g., by covering blind spots or providing diversity reception at a receiving node. In particular, passive RIS provide not only an energy-efficient solution but also a cost-effective one both in terms of the initial deployment cost and the operational costs. RIS are promising to be deployed in a wide



Fig. 1: Filling the coverage gap in mmWave communications by utilizing Reconfigurable Intelligent Surfaces enabled by multi-beamforming

range of communications scenarios and use-cases, such as high throughput MIMO communications[4][5], ad-hoc networks, e.g., UAV communications[6], physical layer security[7], etc. Apart from the works focusing on theoretical performance analysis of RIS-enabled systems [8][5][9], considerable amount of work has been dedicated to optimizing such an integration, mostly focusing on the phase optimization of RIS elements [10][11][12][13] to achieve various goals such as maximum received signal strength, maximum spectral efficiency, etc. For more information on RIS, we refer the interested readers to [14] and the references therein.

In this paper, we consider a communication scenario between a transmitter, e.g., the base station (BS), and terrestrial end-users through a passive RIS that reflects the received signal from the transmitter towards the users. Hence, the users that are otherwise in blind spots of network coverage, become capable of communicating with the base station through the RIS that is serving as a passive reflector (passive relay) maintaining communication links to the BS and to the users. Given the geo-spatial variance among the locations of the end-users served by the same wireless system, the RIS may have to accommodate users that lie in distant angular intervals simultaneously, with satisfactory quality of service (QoS). In what we refer to as *multi-beamforming*, we particularly address the design of beams

consisting of multiple disjoint lobes using RIS in order to cover different blind spots using sharp and effective beam patterns. In the following, we summarize the main contributions of this paper:

- We design the parameters of the RIS to achieve multiple disjoint beams covering various ranges of solid angle. The designed beams are fairly sharp, have almost uniform gain in the desired angular coverage interval (ACI), and have negligible power transmitted outside the ACI.
- We formulate the multi-beamforming design as an optimization problem for which we derive the optimal solution.
- Thanks to the derived analytical closed form solutions for the optimal multi-beamforming design, the proposed solution bears very low computational complexity even for RIS with massive array size.
- Through numerical evaluation we show that by using passive RIS, multi-beamforming can simultaneously cover multiple ACIs. Moreover, multi-beamforming provides tens of dB power boost w.r.t. single-beam RIS design even when the single beam is designed optimally.

Notation Throughout this paper, \mathbb{C} , \mathbb{R} , and \mathbb{Z} denote the set of complex, real, and integer numbers, respectively, $\mathcal{CN}(m, \sigma^2)$ denotes the circularly symmetric complex normal distribution with mean m and variance σ^2 , $[a, b]$ is the closed interval between a and b , $\mathbf{1}_{a,b}$ is the $a \times b$ all ones matrix, \mathbf{I}_N is the $N \times N$ identity matrix, $\mathbb{1}_{[a,b]}$ is the indicator function, $\|\cdot\|$ is the 2-norm, $\|\cdot\|_\infty$ is the infinity-norm, $|\cdot|$ may denote cardinality if applied to a set and 1-norm if applied to a vector, \odot is the Hadamard product, \otimes is the Kronecker product, \mathbf{A}^H , and $\mathbf{A}_{a,b}$ denote conjugate transpose, and $(a, b)^{th}$ entry of \mathbf{A} respectively.

The remainder of the paper is organized as follows. Section II describes the system model. In Section III we formulate the multi-beamforming design problem and propose our solutions in Section IV. Section V presents our evaluation results, and finally, we conclude in Section VI.

II. SYSTEM MODEL

A. Channel Model

Consider a communication system consisting of a multi-antenna BS with M_t antenna elements as a transmitter and a multi-antenna receiver with M_r antenna elements. The MIMO system is aided by a multi-element RIS consisting of M elements arranged in $M_h \times M_v$ grid in the form of UPA as shown in figure 1 where M_h and M_v are the number of elements in the horizontal and vertical directions, respectively. The received signal $\mathbf{y} \in \mathbb{C}^{M_r}$ as a function of the transmitted signal $\mathbf{x} \in \mathbb{C}^{M_t}$ can be written as,

$$\mathbf{y} = (\mathbf{H}_r \Theta \mathbf{H}_t) \mathbf{x} + \mathbf{z} \quad (1)$$

where \mathbf{z} is the noise vector, with each element of \mathbf{z} drawn from a complex Gaussian distribution $\mathcal{CN}(0, \sigma_n^2)$, $\mathbf{H}_t \in \mathbb{C}^{M \times M_t}$ and $\mathbf{H}_r \in \mathbb{C}^{M_r \times M}$ are the channel matrices between each party and the RIS. We assume that the RIS consists of elements

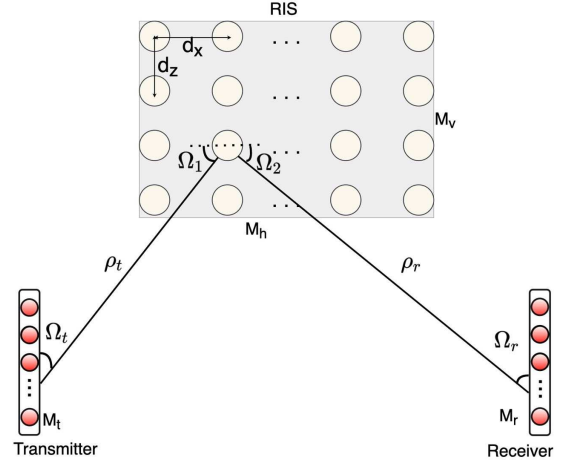


Fig. 2: System Model

for which both the phase θ_m and the gain β_m (in form of attenuation of the reflected signal) of each element, say m , may be controlled and $\Theta \in \mathbb{C}^{M \times M}$ is a diagonal matrix where the element (m, m) denotes the coefficient $\beta_m e^{j\theta_m}$ of the m^{th} element of the RIS. Assuming LoS channel model both between the transmitter and the RIS and between the RIS and the receiver and using the directivity vectors at the transmitter, the RIS, and the receiver, the effective channel matrices can be written as,

$$\mathbf{H}_r = \mathbf{a}_{M_r}(\Omega_r) \rho_r \mathbf{a}_M^H(\Omega_2) \quad (2)$$

$$\mathbf{H}_t = \mathbf{a}_M(\Omega_1) \rho_t \mathbf{a}_{M_t}^H(\Omega_t) \quad (3)$$

where $\mathbf{a}_M(\Omega)$ is the array response vector of an RIS with elements in a UPA structure (RIS-UPA), Ω_t and Ω_2 are the solid angles of departure (AoD) of the transmitted beams from transmitter and the RIS and Ω_1 and Ω_r are the solid angle of arrival (AoA) of the received beams at the RIS and the receiver, respectively. The gain of the LoS paths from the transmitter to the RIS and from the RIS to the receiver are denoted by ρ_t and ρ_r , respectively. Note that the solid angle Ω_a specifies a pair of elevation and azimuth angles i.e. (ϕ_a, θ_a) , $a \in \{1, 2, t, r\}$. Further, assuming no pairing between the RIS elements, Θ will be a diagonal matrix specified as

$$\Theta = \text{diag}\{\beta_1 e^{j\theta_1}, \dots, \beta_M e^{j\theta_M}\} \quad (4)$$

where $\beta_i \in [0, 1]$ and $\theta_i \in [0, 2\pi]$.

B. RIS Model

Suppose an RIS consisting of $M_h \times M_v$ antenna elements forming a UPA structure is placed at the x - z plane, where $M = M_h M_v$ and z axis corresponds to horizon. Let d_z , and d_x denote the distance between the antennas elements in z and x axis, respectively. The directivity of a RIS-UPA can be found in similar way to that of a UPA. At a solid angle $\Omega = (\phi, \theta)$, we have,

$$\mathbf{a}_M(\Omega) = \left[1, e^{j \frac{2\pi}{\lambda} \mathbf{r}_\Omega \mathbf{r}_1}, \dots, e^{j \frac{2\pi}{\lambda} \mathbf{r}_\Omega \mathbf{r}_{M-1}} \right]^T \in \mathbb{C}^M \quad (5)$$

where respectively, $\mathbf{r}_\Omega = [\cos \phi \cos \theta, \cos \phi \sin \theta, \sin \phi]$, and $\mathbf{r}_m = (m_h d_x, 0, m_v d_z)$ denote the direction corresponding to the solid angle Ω and the location of the m -th RIS element corresponding to the antenna placed at the position (m_v, m_h) . Further, we define a transformation of variables as follows. For a solid angle $\Omega = [\phi, \theta]$, define $\psi = [\xi, \zeta]$ as follows,

$$\xi = \frac{2\pi d_z}{\lambda} \sin \phi, \quad \zeta = \frac{2\pi d_x}{\lambda} \sin \theta \cos \phi \quad (6)$$

Introducing the new variables into equation (5), it is straightforward to write,

$$\mathbf{a}_M(\Omega) = \mathbf{d}_M(\xi, \zeta) = \mathbf{d}_{M_v}(\xi) \otimes \mathbf{d}_{M_h}(\zeta) \in \mathbb{C}^M \quad (7)$$

where we define for $a \in \{v, h\}$ the directivity vectors \mathbf{d}_{M_a} as follows, and denote by \mathbf{d}_M the directivity vector corresponding to the RIS.

$$\begin{aligned} \mathbf{d}_{M_v}(\xi) &= \left[1, e^{j\xi} \dots e^{j(M_v-1)\xi}\right]^T \in \mathbb{C}^{M_v} \\ \mathbf{d}_{M_h}(\zeta) &= \left[1, e^{j\zeta} \dots e^{j(M_h-1)\zeta}\right]^T \in \mathbb{C}^{M_h} \end{aligned} \quad (8)$$

Let \mathcal{B} be the angular range under cover defined as

$$\mathcal{B} \doteq [-\phi^B, \phi^B] \times [-\theta^B, \theta^B] \quad (9)$$

We note that there is a one-to-one correspondence between the solid angle $\Omega = (\phi, \psi)$ and its representation after change of variable as (ζ, ξ) . Accordingly, let \mathcal{B}^ψ be the angular range under cover in the (ζ, ξ) domain given by

$$\mathcal{B}^\psi \doteq [-\xi^B, \xi^B] \times [-\zeta^B, \zeta^B] \quad (10)$$

In this paper, we set $d_x = d_z = \frac{\lambda}{2}$, $\phi^B = \frac{\pi}{4}$, and $\theta^B = \frac{\pi}{2}$, hence $\xi \in [-\pi\frac{\sqrt{2}}{2}, \pi\frac{\sqrt{2}}{2}]$, and $\zeta \in [-\pi, \pi]$. Note that, the dependence between variables ξ and ζ can be resolved using the approximation in [15]. Let us uniformly divide \mathcal{B}^ψ into $Q = Q_v Q_h$ subregions, where Q_h and Q_v are the number of division in horizontal and vertical directions, respectively. A subregion is denoted by

$$\mathcal{B}_{p,q}^\psi \doteq \nu_v^{p,q} \times \nu_h^{p,q}$$

where $\nu_v^p = [\zeta^{p-1}, \zeta^p]$, and $\nu_h^q = [\xi^{q-1}, \xi^q]$ defining,

$$\xi^p = -\xi^B + p\delta_v, \quad \zeta^q = -\zeta^B + q\delta_h \quad (11)$$

with $\delta_v = \frac{2\xi^B}{Q_v}$, and $\delta_h = \frac{2\zeta^B}{Q_h}$. In the next section, we define the multi-beamforming design problem as the core of our proposed RIS structure.

III. PROBLEM FORMULATION

Prior to formulating the multi-beamforming design problem, we proceed with a few preliminary definitions. Let us define the *multi-beam* $\mathcal{D} = (\mathcal{D}_1, \dots, \mathcal{D}_k)$ as collection of k compound beams $\mathcal{D}_i, i = 1, \dots, k$ where $\mathcal{D}_i \subseteq \mathcal{B}^\psi$ and $\mathcal{D}_i = \bigcup_{(p,q) \in \mathcal{A}_i} \mathcal{B}_{p,q}^\psi$, with \mathcal{A}_i being the set of all pairs (p, q) that all beams $\mathcal{B}_{p,q}^\psi$ cover \mathcal{D}_i . The union of $\mathcal{B}_{p,q}^\psi$ is in fact approximating the shape of the solid angle for the desired compound beam corresponding to \mathcal{D}_i . By using larger number

of division, i.e., finer beams, one can make the approximation better. We have

$$\mathcal{A}_i = \underset{\{\hat{\mathcal{A}}|\mathcal{D}_i \subseteq \bigcup_{(p,q) \in \mathcal{A}} \mathcal{B}_{p,q}\}}{\text{arg min}} |\hat{\mathcal{A}}| \quad (12)$$

Further define $\mathcal{A} = \bigcup_{i=1}^k \mathcal{A}_i$. We aim to design a beamforming vector \mathbf{c} such that the multi-beam \mathcal{D} is covered when the RIS is excited by an incident wave received at solid angle Ω_1 . Using (1)-(3), the contribution of the RIS in the channel matrix for a receiver at the solid angle Ω_2 is given by

$$\Gamma = \mathbf{a}_M^H(\Omega_2) \Theta \mathbf{a}_M(\Omega_1) = \mathbf{d}_M^H(\Omega_2) \boldsymbol{\lambda} \quad (13)$$

where $\boldsymbol{\lambda} \in \mathbb{C}^M$ is defined as follows. For antenna element located at position (m_v, m_h) in the UPA grid, we have

$$\lambda_{m_v, m_h} = \beta_{m_v, m_h} e^{-j(\theta_{m_v, m_h} - m_v \xi_1 - m_h \zeta_1)} \quad (14)$$

where (ξ_1, ζ_1) is the representation of Ω_1 in the ψ -domain, and hence the vector $\boldsymbol{\lambda}$ is given by

$$\boldsymbol{\lambda} = [\lambda_{0,0}, \dots, \lambda_{0, M_h-1}, \lambda_{1,0}, \dots, \lambda_{M_v-1, M_h-1}] \quad (15)$$

We note that $\boldsymbol{\lambda}$ depends on the AoA of the incident beams at the RIS, i.e., Ω_1 , as well as the RIS parameters. The reference gain of RIS in direction (ζ, ξ) in terms of $\boldsymbol{\lambda}$ is given by

$$G(\xi, \zeta, \boldsymbol{\lambda}) = \left| (\mathbf{d}_{M_v}(\xi) \otimes \mathbf{d}_{M_h}(\zeta))^H \boldsymbol{\lambda} \right|^2 \quad (16)$$

On the other hand, the gain of UPA antenna with the feed coefficients \mathbf{c} is given by

$$G(\xi, \zeta, \mathbf{c}) = \left| (\mathbf{d}_{M_v}(\xi) \otimes \mathbf{d}_{M_h}(\zeta))^H \mathbf{c} \right|^2 \quad (17)$$

that has a clear similarity. This means that to design the RIS-UPA for the STMR problem with receive zone \mathcal{D} we can use the multi-beamforming design framework to cover the ACI's included in \mathcal{D} for the UPA antenna. In particular, a RIS-UPA with parameters $\boldsymbol{\lambda}$ and a UPA-antenna with beamforming parameters \mathbf{c} have the same beamforming gain pattern if UPA structures are the same and $\boldsymbol{\lambda} = \mathbf{c}$. Hence, a RIS-UPA which is excited from the solid angle Ω_1 has the same beamforming gain as its UPA antenna counterpart if $\Theta = \text{diag}\{\mathbf{c}^T \odot \mathbf{a}_M^H(\Omega_1)\}$. For any normalized beamforming vector \mathbf{c} , it is straightforward to show that,

$$\int_{-\pi}^{\pi} \int_{-\pi}^{\pi} G(\xi, \zeta, \mathbf{c}) d\xi d\zeta = (2\pi)^2 \quad (18)$$

We wish to design beamformers that provide high, sharp, and constant gain within the desired ACI's and zero gain everywhere else. We have then for the ideal gain corresponding to such beamformer \mathbf{c} that,

$$\begin{aligned} \iint_{\mathcal{B}^\psi} G_{\mathcal{D}}^{\text{ideal}}(\xi, \zeta) d\xi d\zeta &= \sum_{i=1}^k \iint_{\mathcal{D}_i} t d\xi d\zeta \\ &= \sum_{(p,q) \in \mathcal{A}} \iint_{\mathcal{B}_{p,q}^\psi} t d\xi d\zeta = \sum_{(p,q) \in \mathcal{A}} \delta_{p,q} t = (2\pi)^2 \end{aligned} \quad (19)$$

where $\delta_{p,q}$ denotes the area of the (p, q) -th beam in the (ξ, ζ) domain. Therefore, we can derive $t = \frac{(2\pi)^2}{|\mathcal{A}|\delta_{p,q}}$. It holds that,

$$G_{\mathcal{D}}^{\text{ideal}}(\xi, \zeta) = \frac{(2\pi)^2}{|\mathcal{A}|\delta_{p,q}} \mathbf{1}_{\mathcal{D}}(\xi, \zeta) \quad (20)$$

Using the beamformer \mathbf{c} we wish to mimic the deal gain in equation (20). Therefore, we formulate the following optimization problem,

$$\mathbf{c}_{\mathcal{D}}^{\text{opt}} = \arg \min_{\mathbf{c}, \|\mathbf{c}\|=1} \iint_{\mathcal{B}^{\psi}} |G_{\mathcal{D}}^{\text{ideal}}(\xi, \zeta) - G(\xi, \zeta, \mathbf{c})| d\xi d\zeta \quad (21)$$

By partitioning the range of (ξ, ζ) into the pre-defined intervals, and then uniformly sampling with the rate (L_v, L_h) per interval along both axis, we can rewrite the optimization problem as follows,

$$\begin{aligned} \mathbf{c}_{\mathcal{D}}^{\text{opt}} &= \arg \min_{\mathbf{c}, \|\mathbf{c}\|=1} \sum_{r=1}^{Q_v} \sum_{s=1}^{Q_h} \iint_{\mathcal{B}_{r,s}^{\psi}} |G_{\mathcal{D}}^{\text{ideal}}(\xi, \zeta) - G(\xi, \zeta, \mathbf{c})| d\xi d\zeta \\ &= \lim_{L_h, L_v \rightarrow \infty} \sum_{r=1}^{Q_v} \sum_{s=1}^{Q_h} \sum_{l_v=1}^{L_v} \sum_{l_h=1}^{L_h} \\ &\quad \frac{\delta_v \delta_h}{L_h L_v} |G_{\mathcal{D}}^{\text{ideal}}(\xi_{r,l_v}, \zeta_{s,l_h}) - G(\xi_{r,l_v}, \zeta_{s,l_h}, \mathbf{c})| \end{aligned} \quad (22)$$

where,

$$\xi_{r,l_v} = \xi^{r-1} + l_v \frac{\delta_v}{L_v}, \quad \zeta_{s,l_h} = \zeta^{s-1} + l_h \frac{\delta_h}{L_h} \quad (23)$$

with $\delta_a = \frac{2\psi^B}{Q_a}$, for $a \in \{v, h\}$. Note that it holds for all (p, q) pairs that, $\delta_{p,q} = \delta_v \delta_h$. We can rewrite equation (22) as,

$$\mathbf{c}_{\mathcal{D}}^{\text{opt}} = \arg \min_{\mathbf{c}, \|\mathbf{c}\|=1} \lim_{L_h, L_v \rightarrow \infty} \frac{1}{L_h L_v} |G_{\mathcal{D}}^{\text{ideal}} - \mathbf{G}(\mathbf{c})| \quad (24)$$

where,

$$\mathbf{G}(\mathbf{c}) = \delta_{p,q} [G(\xi_{1,1}, \zeta_{1,1}, \mathbf{c}) \cdots G(\xi_{Q_v, L_v}, \zeta_{Q_h, L_h}, \mathbf{c})]^T \quad (25)$$

and,

$$\mathbf{G}_{\mathcal{D}}^{\text{ideal}} = \delta_{p,q} [G_{\mathcal{D}}^{\text{ideal}}(\xi_{1,1}, \zeta_{1,1}) \cdots G_{\mathcal{D}}^{\text{ideal}}(\xi_{Q_v, L_v}, \zeta_{Q_h, L_h})]^T \quad (26)$$

Unfortunately, the optimization problem in (24) does not admit an optimal closed-form solution as is, due to the absolute values of the complex numbers existing in the formulation. However, note that,

$$\begin{aligned} \mathbf{G}_{\mathcal{D}}^{\text{ideal}} &= \sum_{(p,q) \in \mathcal{A}} \delta_{p,q} \frac{(2\pi)^2}{|\mathcal{A}|\delta_{p,q}} (\mathbf{e}_{p,q} \otimes \mathbf{1}_{L,1}) \\ &= \frac{(2\pi)^2}{|\mathcal{A}|} \sum_{(p,q) \in \mathcal{A}} \mathbf{e}_{p,q} \otimes \mathbf{1}_{L,1} \end{aligned} \quad (27)$$

with $\mathbf{e}_{p,q} \in \mathbb{Z}^Q$ being the standard basis vector for the (p, q) -th axis among (Q_v, Q_h) pairs. Now, note that $\mathbf{1}_{L,1} = \mathbf{g} \odot \mathbf{g}^*$ for any equal gain $\mathbf{g} \in \mathbb{C}^L$ where $L = L_h L_v$. An equal-gain vector

$\mathbf{g} \in \mathbb{C}^L$ is a vector where all elements have equal absolute values (in this case, equal to 1). Therefore, we can write:

$$\begin{aligned} \mathbf{G}_{\mathcal{D}}^{\text{ideal}} &= \sum_{(p,q) \in \mathcal{A}} \frac{(2\pi)^2}{|\mathcal{A}|} (\mathbf{e}_{p,q} \otimes (\mathbf{g} \odot \mathbf{g}^*)) \\ &= \frac{(2\pi)^2}{|\mathcal{A}|} \sum_{(p,q) \in \mathcal{A}} (\mathbf{e}_{p,q} \otimes \mathbf{g}) \odot (\mathbf{e}_{p,q} \otimes \mathbf{g})^* \\ &= \left(\sum_{(p,q) \in \mathcal{A}} \frac{2\pi}{\sqrt{|\mathcal{A}|}} (\mathbf{e}_{p,q} \otimes \mathbf{g}) \right) \\ &\quad \odot \left(\sum_{(p,q) \in \mathcal{A}} \frac{2\pi}{\sqrt{|\mathcal{A}|}} (\mathbf{e}_{p,q} \otimes \mathbf{g}) \right)^* \end{aligned} \quad (28)$$

Also, it is straightforward to write,

$$\mathbf{G}(\mathbf{c}) = (\mathbf{D}^H \mathbf{c}) \odot (\mathbf{D}^H \mathbf{c})^* \quad (29)$$

where, $\mathbf{D}^H = \sqrt{\delta_v \delta_h} (\mathbf{D}_v^H \otimes \mathbf{D}_h^H)$, and for $a \in \{v, h\}$, and $b = 1 \dots Q_a$ we have,

$$\mathbf{D}_a = [\mathbf{D}_{a,1}, \dots, \mathbf{D}_{a,Q_a}] \in \mathbb{C}^{M_a \times L_a Q_a} \quad (30)$$

where,

$$\mathbf{D}_{v,b} = [\mathbf{d}_{M_v}(\xi_{b,1}), \dots, \mathbf{d}_{M_v}(\xi_{b,L_v})] \in \mathbb{C}^{M_v \times L_v} \quad (31)$$

$$\mathbf{D}_{h,b} = [\mathbf{d}_{M_h}(\zeta_{b,1}), \dots, \mathbf{d}_{M_h}(\zeta_{b,L_h})] \in \mathbb{C}^{M_h \times L_h} \quad (32)$$

Comparing the expressions (24), (28), and (29), one can show that the optimal choice of $\mathbf{c}_{\mathcal{D}}$ in (21) is the solution to the following optimization problem for proper choices of $\mathbf{g}_{p,q}$.

Problem 1. Given equal-gain vectors $\mathbf{g}_{p,q} \in \mathbb{C}^L$, for $(p, q) \in \mathcal{A}$ find a vector $\mathbf{c}_{\mathcal{D}} \in \mathbb{C}^M$ such that

$$\begin{aligned} \mathbf{c}_{\mathcal{D}} &= \arg \min_{\mathbf{c}, \|\mathbf{c}\|=1} \\ &\quad \lim_{L \rightarrow \infty} \left\| \sum_{(p,q) \in \mathcal{A}} \frac{2\pi}{\sqrt{|\mathcal{A}|}} (\mathbf{e}_{p,q} \otimes \mathbf{g}_{p,q}) - \mathbf{D}^H \mathbf{c} \right\|^2 \end{aligned} \quad (33)$$

However, we now need to find the optimal choices of $\mathbf{g}_{p,q}$ that minimize the objective in (24). Using (28), and (29), we have the following optimization problem.

Problem 2. Find equal-gain vectors $\mathbf{g}_{p,q}^* \in \mathbb{C}^L$, $(p, q) \in \mathcal{A}$ such that

$$\begin{aligned} \langle \mathbf{g}_{p,q}^* \rangle_{(p,q) \in \mathcal{A}} &= \arg \min_{\langle \mathbf{g}_{p,q} \rangle_{(p,q) \in \mathcal{A}}} \\ &\quad \left\| \text{abs}(\mathbf{D}^H \mathbf{c}_{\mathcal{D}}) - \frac{2\pi}{\sqrt{|\mathcal{A}|}} \text{abs} \left(\sum_{(p,q) \in \mathcal{A}} \mathbf{e}_{p,q} \otimes \mathbf{g}_{p,q} \right) \right\|^2 \end{aligned} \quad (34)$$

where $\text{abs}(\cdot)$ denotes the element-wise absolute value of a vector.

Next, we continue with the solution of Problems 1, and 2.

IV. PROPOSED MULTI-BEAM DESIGN

Note that the solution to problem 1 is the limit of the sequence of solutions to a least-square optimization problem as L goes to infinity. For each L we find that,

$$\mathbf{c}_{\mathcal{D}}^{(L)} = \sum_{(p,q) \in \mathcal{A}} \frac{2\pi}{\sqrt{|\mathcal{A}|}} (\mathbf{D}\mathbf{D}^H)^{-1} \mathbf{D} (\mathbf{e}_{p,q} \otimes \mathbf{g}_{p,q}) \quad (35)$$

$$\mathbf{c}_{\mathcal{D}}^{(L)} = \sum_{(p,q) \in \mathcal{A}} \sigma \mathbf{D}_{p,q} \mathbf{g}_{p,q} \quad (36)$$

where $\sigma = \frac{2\pi\sqrt{\delta_v\delta_h}}{LQ\delta_v\delta_h\sqrt{|\mathcal{A}|}} = \frac{2\pi}{LQ\sqrt{\delta_v\delta_h|\mathcal{A}|}}$, noting that it holds that,

$$\mathbf{D}\mathbf{D}^H = \delta_v\delta_h(\mathbf{D}_v \otimes \mathbf{D}_h)(\mathbf{D}_v^H \otimes \mathbf{D}_h^H) = \delta_v\delta_h LQ \quad (37)$$

Even though Problem 1 admits a nice analytical closed form solution, doing so for the Problem 2 is not a trivial task, especially due to the fact that the objective function is not convex. However, the convexification of the objective problem (34) in the form of

$$\arg \min_{\langle \mathbf{g}_{p,q} \rangle_{(p,q) \in \mathcal{A}}} \left\| \mathbf{D}^H \mathbf{c}_{\mathcal{D}} - \frac{2\pi}{\sqrt{|\mathcal{A}|}} \sum_{(p,q) \in \mathcal{A}} \mathbf{e}_{p,q} \otimes \mathbf{g}_{p,q} \right\|^2 \quad (38)$$

and using $\mathbf{c}_{\mathcal{D}}$ from (36) leads to an effective solution for the original problem. Indeed, it can be verified by solving the optimization problem (38) numerically that a close-to-optimal solution admits the following form.

$$\mathbf{g}_{p,q}^* = \left[1, \alpha_v \alpha_h, \dots, \alpha_v^{(L_v-1)} \alpha_h^{(L_h-1)} \right]^T, (p,q) \in \mathcal{A} \quad (39)$$

for some η_v, η_h where $\alpha_a = e^{j(\frac{\eta_a}{L_a})}$, $a \in \{v, h\}$. In the following, we use the analytical form (39) for $\mathbf{g}_{p,q}^*$ for the rest of our derivations. This solution would not be the optimal solution for the original problem (34). However, it provides a near optimal solution with added benefits of allowing to (i) find the limit of the solution as L goes to infinity, and (ii) express the beamforming vectors in closed form, as it will be revealed in the following discussion. An analytical closed form solution for $\mathbf{c}_{\mathcal{D}}$ can be found as follows. It holds that,

$$\begin{aligned} \mathbf{c}_{\mathcal{D}}^{(L)} &= \sum_{(p,q) \in \mathcal{A}} \left(\sum_{(l_v, l_h) = (1,1)}^{(L_v, L_h)} \sigma g_{p,q, l_v, l_h} \mathbf{d}_{M_t}(\xi_{p, l_v}, \zeta_{q, l_h}) \right) \\ &= \sum_{(p,q) \in \mathcal{A}} \left(\sum_{(l_v, l_h) = (1,1)}^{(L_v, L_h)} \sigma g_{p,q, l_v, l_h} \left[1, \dots, e^{j\mu_{p,q, l_v, l_h}^{M_v-1, M_h-1}} \right]^T \right) \end{aligned} \quad (40)$$

where $\mu_{p,q, l_v, l_h}^{m_v, m_h} = (m_v \xi_{p, l_v} + m_h \zeta_{q, l_h})$. We can then write for the $(m_v, m_h)^{th}$ component of the beamformer $\mathbf{c}_{\mathcal{D}}$,

$$\begin{aligned} c_{p,q, m_v, m_h} &= \lim_{L_h, L_v \rightarrow \infty} \frac{1}{L_h L_v} \sum_{(p,q) \in \mathcal{A}} \sum_{(l_h, l_v) = (1,1)}^{(L_h, L_v)} g_{p,q, l_v, l_h} e^{j\mu_{p,q, l_v, l_h}^{M_v-1, M_h-1}} \end{aligned} \quad (41)$$

Using equation (23), we can rewrite (41) as,

$$c_{p,q, m_v, m_h} = \frac{2\pi}{Q} e^{j\chi_{p-1, q-1}^{m_v, m_h}} \left(\frac{1}{L_v} \lim_{L_v \rightarrow \infty} \sum_{l_v=1}^{L_v} e^{j\frac{\eta_v + m_v \delta_v l_v}{L_v}} \right) \left(\frac{1}{L_h} \lim_{L_h \rightarrow \infty} \sum_{l_h=1}^{L_h} e^{j\frac{\eta_h + m_h \delta_h l_h}{L_h}} \right) \quad (42)$$

to get,

$$\begin{aligned} c_{\mathcal{D}, m_v, m_h} &= \sum_{(p,q) \in \mathcal{A}} \frac{2\pi}{Q} e^{j\chi_{p-1, q-1}^{m_v, m_h}} \int_0^1 e^{j\xi_v x} dx \int_0^1 e^{j\xi_h x} dx \\ &= \sum_{(p,q) \in \mathcal{A}} \frac{2\pi}{Q} e^{j(\zeta_{p-1, q-1}^{m_v, m_h} + \frac{\xi_v + \xi_h}{2})} \text{sinc}\left(\frac{\xi_v}{2\pi}\right) \text{sinc}\left(\frac{\xi_h}{2\pi}\right) \end{aligned} \quad (43)$$

with $\chi_{p,q}^{m_v, m_h} = (m_v \xi^p + m_h \zeta^q)$, and $\xi_a = \delta_a m_a + \eta_a$, for $a \in \{v, h\}$. Now that the closed-form expression for $\mathbf{c}_{\mathcal{D}}$, and therefore, λ is known, the RIS parameters at the antenna placed at location (m_v, m_h) can be easily computed. More precisely, we get,

$$\beta_{m_v, m_h} = |\mathbf{c}_{\mathcal{D}, m_v, m_h}| \quad (44)$$

$$\theta_{m_v, m_h} = \angle \mathbf{c}_{\mathcal{D}, m_v, m_h} + m_v \psi_{v,1} + m_h \psi_{h,1} \quad (45)$$

In the case that gain control (attenuation) at the RIS elements is not feasible, $\beta_{m_v, m_h} = 1$ will be replaced by the derivation for the absolute value of the RIS parameters. Next, we verify the effectiveness of our multi-beamforming design approach by means of numerical experiments.

V. PERFORMANCE EVALUATION

In this section, we evaluate the performance of our multi-beam design framework. We aim to design a dual-beam which comprises of two lobes with centers at $(-8\pi/32, -5\pi/32)$ and $(7\pi/32, \pi/32)$ in the (ϕ, θ) domain, and with the beamwidth equal to $\pi/16$. We divide both the ψ_h , and the ψ_v range uniformly into $Q_h = 16$, and $Q_v = 16$ regions resulting in $Q = 256$ equally-shaped units in (ψ_v, ψ_h) domain. We cover each desired beam with the smallest number of the designed units to provide uniform gain at the desired angular regions. Figures 3(a)-(c) depict the beam pattern of the dual beam obtained through our design where all angles are measured in radians. Figure 3(a), shows the heat-map corresponding to the gain of the reflected beam from RIS for the designed dual-beam. The gains are computed in dB. It can be seen that the designed beamformer generates two disjoint beams with an almost uniform gain over the desired ACIs. It is also observed that the beams sharply drop outside the desired ACIs and effectively suppress the gain everywhere outside ACI. In order to quantify the suppression we depict the cross-section of the gain pattern at a fixed elevation angle ϕ_c for two values of $\phi_c \in \{-8\pi/32, 7\pi/32\}$ located inside the two lobes of the designed dual beam in Figure 3(b). Similarly, Figure 3(c) shows the cross-section of the beam pattern at a fixed azimuth angle θ_c for two values of $\theta_c \in \{-5\pi/32, \pi/32\}$. Both Figures 3(b) and (c) confirm the sharpness of both lobes of

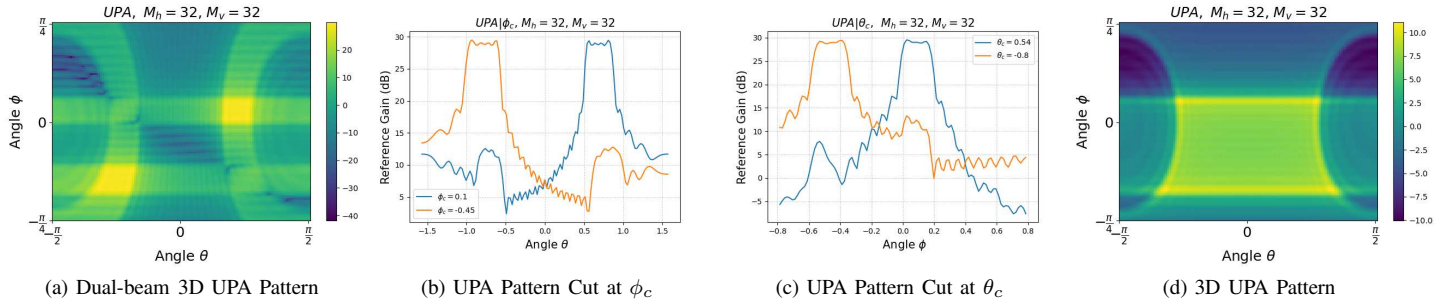


Fig. 3: Beam pattern for UPA structure

the designed dual-beam and can be used to find the beamwidth of each lobes at an arbitrary fraction from its maximum values, e.g., the 3dB beamwidth or 10dB beamwidth. Indeed, there is negligible difference between 3dB and 10dB beamwidth which clarifies the sharpness of the beams. From Figures 3(b) and(c), it is also observed that the gain within the ACI is almost uniform. Nonetheless, we should emphasize the fact that the shape of the lobes of the beam that are centered at different solid angle may suffer from slight deformation as seen by Figure 3(a). This phenomenon worsens as the corresponding lobes of the beams get too close to the plane of the RIS.

Finally, in order to compare the performance of our multi-beam design to a single-beam design, we consider a beam with single lobe which is capable of covering the same two regions as in the dual-beam design. Figure 3(d), shows the heat-map corresponding to the gain of the reflected beam from RIS for the corresponding single beam that is optimized based on our design. As it was the case for multi-beam, this figure also shows that for a single beam our design generates an almost uniform and fairly sharp beam. However, comparing Figures 3(a) and(d), we observe that in the desired ACI, the multi-beamforming procedure, enhances the gain by about 20 dB over the beams with optimized single lobe.

VI. CONCLUSIONS

RIS can be incorporated into mmWave communications to fill the coverage gaps in the blind-spots of the mmWave system. We proposed a novel approach for designing RIS employing a UPA antenna structure, that is capable of covering multiple disjoint angular intervals simultaneously. Both our theoretical results and numerical experiments demonstrate that our technique termed as multi-beamforming will result in sharp, high, and stable gains within the desired ACI's regardless of their spatial locations, while effectively, suppressing all the undesired out-of-band components.

REFERENCES

- [1] C. Huang, A. Zappone, G. C. Alexandropoulos, M. Debbah, and C. Yuen, "Reconfigurable intelligent surfaces for energy efficiency in wireless communication," *IEEE Transactions on Wireless Communications*, vol. 18, no. 8, pp. 4157–4170, 2019.
- [2] C. Liaskos, S. Nie, A. Tsioliaridou, A. Pitsillides, S. Ioannidis, and I. Akyildiz, "A new wireless communication paradigm through software-controlled metasurfaces," *IEEE Communications Magazine*, vol. 56, no. 9, pp. 162–169, 2018.
- [3] E. Basar, M. Di Renzo, J. De Rosny, M. Debbah, M.-S. Alouini, and R. Zhang, "Wireless communications through reconfigurable intelligent surfaces," *IEEE Access*, vol. 7, pp. 116 753–116 773, 2019.
- [4] C. Huang, R. Mo, and C. Yuen, "Reconfigurable intelligent surface assisted multiuser mimo systems exploiting deep reinforcement learning," *IEEE Journal on Selected Areas in Communications*, vol. 38, no. 8, pp. 1839–1850, 2020.
- [5] Q. Nadeem, A. Kammoun, A. Chaaban, M. Debbah, and M.-S. Alouini, "Asymptotic max-min sinr analysis of reconfigurable intelligent surface assisted mimo systems," *IEEE Transactions on Wireless Communications*, vol. 19, no. 12, pp. 7748–7764, 2020.
- [6] S. Li, B. Duo, X. Yuan, Y.-C. Liang, and M. Di Renzo, "Reconfigurable intelligent surface assisted uav communication: Joint trajectory design and passive beamforming," *IEEE Wireless Communications Letters*, vol. 9, no. 5, pp. 716–720, 2020.
- [7] A. U. Makarfi, K. M. Rabie, O. Kaiwartya, X. Li, and R. Kharel, "Physical layer security in vehicular networks with reconfigurable intelligent surfaces," in *2020 IEEE 91st Vehicular Technology Conference (VTC2020-Spring)*, 2020, pp. 1–6.
- [8] Y. Han, W. Tang, S. Jin, C.-K. Wen, and X. Ma, "Large intelligent surface-assisted wireless communication exploiting statistical csi," *IEEE Trans. on Vehicular Tech.*, vol. 68, no. 8, pp. 8238–8242, 2019.
- [9] M. Jung, W. Saad, Y. Jang, G. Kong, and S. Choi, "Performance analysis of large intelligent surfaces (liss): Asymptotic data rate and channel hardening effects," *IEEE Transactions on Wireless Communications*, vol. 19, no. 3, pp. 2052–2065, 2020.
- [10] S. Abeywickrama, R. Zhang, Q. Wu, and C. Yuen, "Intelligent reflecting surface: Practical phase shift model and beamforming optimization," *IEEE Trans. on Comm.*, vol. 68, no. 9, pp. 5849–5863, 2020.
- [11] H. Guo, Y.-C. Liang, J. Chen, and E. G. Larsson, "Weighted sum-rate maximization for reconfigurable intelligent surface aided wireless networks," *IEEE Transactions on Wireless Communications*, vol. 19, no. 5, pp. 3064–3076, 2020.
- [12] B. Di, H. Zhang, L. Li, L. Song, Y. Li, and Z. Han, "Practical hybrid beamforming with finite-resolution phase shifters for reconfigurable intelligent surface based multi-user communications," *IEEE Transactions on Vehicular Technology*, vol. 69, no. 4, pp. 4565–4570, 2020.
- [13] S. Atapattu, R. Fan, P. Dharmawansa, G. Wang, J. Evans, and T. A. Tsiftsis, "Reconfigurable intelligent surface assisted two-way communications: Performance analysis and optimization," *IEEE Transactions on Communications*, vol. 68, no. 10, pp. 6552–6567, 2020.
- [14] Y. Liu, X. Liu, X. Mu, T. Hou, J. Xu, M. Di Renzo, and N. Al-Dhahir, "Reconfigurable intelligent surfaces: Principles and opportunities," *IEEE Communications Surveys Tutorials*, pp. 1–1, 2021.
- [15] J. Song, J. Choi, and D. J. Love, "Common codebook millimeter wave beam design: Designing beams for both sounding and communication with uniform planar arrays," *IEEE Transactions on Communications*, vol. 65, no. 4, pp. 1859–1872, 2017.